Geochemistry Geophysics Geosystems G3
AN ELECTRONIC JOURNAL OF THE EARTH SCIENCES
Published by AGU and the Geochemical Society

Data Brief
Volume 10, Number 8
15 August 2009
Q08011, doi:10.1029/2009GC002451
ISSN: 1525-2027

Click Here for Full Article

Broadband calibration of the R/V *Marcus G. Langseth* four-string seismic sources

M. Tolstoy, J. Diebold, L. Doermann, S. Nooner, and S. C. Webb
Lamont-Doherty Earth Observatory, Earth Institute at Columbia University, 61 Route 9W, Palisades, New York 10964-8000, USA (tolstoy@ldeo.columbia.edu)

D. R. Bohnenstiehl
Department of Marine, Earth and Atmospheric Sciences, North Carolina State University, Raleigh, North Carolina 27695-8208, USA

T. J. Crone and R. C. Holmes
Lamont-Doherty Earth Observatory, Earth Institute at Columbia University, 61 Route 9W, Palisades, New York 10964-8000, USA

[1] The R/V *Marcus G. Langseth* is the first 3-D seismic vessel operated by the U.S. academic community. With up to a four-string, 36-element source and four 6-km-long solid state hydrophone arrays, this vessel promises significant new insights into Earth science processes. The potential impact of anthropogenic sound sources on marine life is an important topic to the marine seismic community. To ensure that operations fully comply with existing and future marine mammal permitting requirements, a calibration experiment was conducted in the Gulf of Mexico in 2007–2008. Results are presented from deep (~1.6 km) and shallow (~50 m) water sites, obtained using the full 36-element (6600 cubic inches) seismic source. This array configuration will require the largest safety radii, and the deep and shallow sites provide two contrasting operational environments. Results show that safety radii and the offset between root-mean-square and sound exposure level measurements were highly dependent on water depth.

Components: 5618 words, 14 figures, 1 table.

Keywords: calibration; Langseth; seismic.

Index Terms: 0935 Exploration Geophysics: Seismic methods (3025, 7294); 3025 Marine Geology and Geophysics: Marine seismics (0935, 7294).

Received 23 February 2009; **Revised** 8 June 2009; **Accepted** 24 June 2009; **Published** 15 August 2009.

Tolstoy, M., J. Diebold, L. Doermann, S. Nooner, S. C. Webb, D. R. Bohnenstiehl, T. J. Crone, and R. C. Holmes (2009), Broadband calibration of the R/V *Marcus G. Langseth* four-string seismic sources, *Geochem. Geophys. Geosyst.*, *10*, Q08011, doi:10.1029/2009GC002451.

1. Introduction

[2] Anthropogenic sound in the marine environment is an area of increasing concern for the conservation of marine animals [e.g., *Tyack*, 2008]. As a result, the marine seismic community, which uses acoustic energy to image the structure of the crust and upper mantle, has come under increased scrutiny [e.g., *Gordon et al.*, 2004]. In an effort to better understand and mitigate the impacts

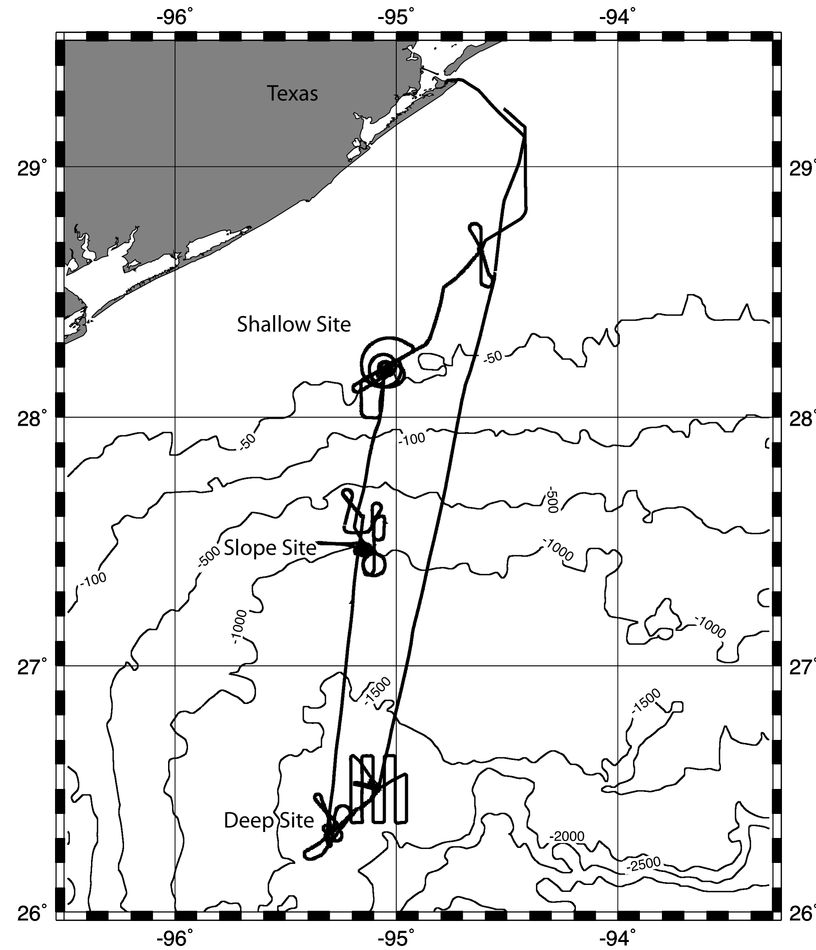

Figure 1. Experiment location map. Ship track shown is from cruise MGL0802, which conducted work at the deep, slope, and shallow sites (from south to north). MGL0707 worked only at the shallow site, in the same location as ML0802. The majority of the shallow site data shown here were collected during MGL0802.

of such activity, the academic community has been working to quantify potential exposure levels through a combination of in situ field recordings and numerical modeling [e.g., *Tolstoy et al.*, 2004; *Breitzke et al.*, 2008; *Tashmukhambetov et al.*, 2008]. In the case of R/V *Ewing* [*Tolstoy et al.*, 2004], which was operated by the U.S. academic community until early 2007, calibration results were utilized in meeting permitting requirements for the vessel's operations.

[3] At the urging of the U.S. academic marine seismic community, the National Science Foundation brought a vessel capable of acquiring 3-D seismic data, the R/V *Marcus G. Langseth*, into academic service in 2008. The ship is operated by the Lamont-Doherty Earth Observatory of Columbia University. As subseafloor structures can be mapped in much finer detail, the addition of 3-D capabilities within the academic community should provide significant new geological insights. Moreover, as 3-D operations will deploy four hydrophone arrays simultaneously, there is a fourfold increase in the amount of data collected per seismic "shot," and eightfold overall, since two sources can be towed in parallel. This increase in efficiency is accommodated without any increase in the source level of the array; in fact, the 3-D source level is half that used for 2-D and refraction surveys.

[4] The seismic source used on the R/V *Langseth* is significantly different from that used on the R/V *Ewing* requiring an updated calibration effort to ensure marine mammal protection. It consists of up to four identical linear subarrays, or strings, whereas the R/V *Ewing* array comprised between 6 and 20 separately towed air guns. For both arrays, tuning is achieved by the inclusion of air guns of varying sizes, each simultaneously producing a bubble whose initial expansion is followed by reverberations with periods that vary according to size. However, the R/V *Langseth*'s subarrays in-

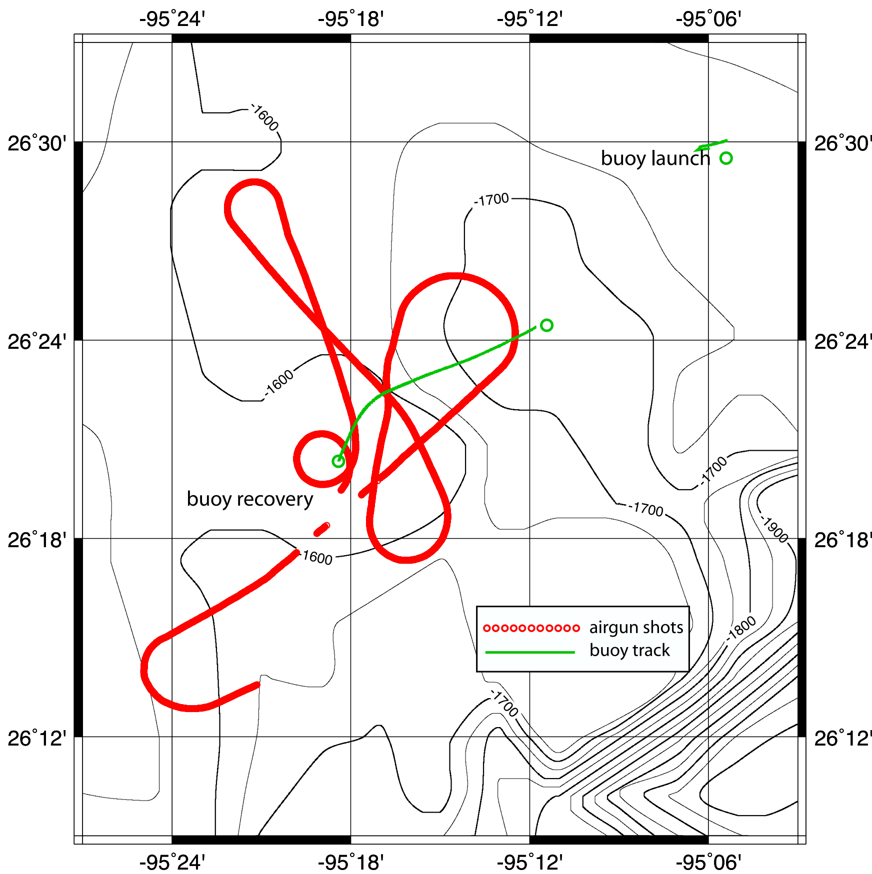

Figure 2. Site map for deep calibration with bathymetry contours at 50 m intervals. The locations of shots recorded are shown in red, and the buoy track is shown in green. Note the buoy was drifting with prevailing currents and winds and so shot tracks were adjusted underway to account for this. The locations of the buoy at deployment, start of shot line, and recovery are illustrated with green circles.

clude several two-gun clusters, which produce less reverberation and may be towed at a more consistent depth. This produces a signal exhibiting a sharper-onset and shorter-duration pulse, with relatively little residual reverberation.

2. Experiment

[5] During two cruises (MGL0707 and MGL0802) in December 2007 and January–February 2008, we recorded more than 13,000 shots on a two-hydrophone spar buoy deployed at shallow, sloped and deep sites in the Gulf of Mexico (Figure 1). The purpose of the experiment was to determine broadband received levels at a range of distances from the seismic array configurations most commonly used on the vessel. The received levels presently defined by the National Marine Fisheries Service as safety criteria (intended to avoid risk of auditory impairment or injury) for pinnipeds and cetaceans are 190 and 180 dB referenced to 1 μPa (RMS), respectively, with 160 dB referenced to 1 μPa (RMS) identified as the level above which (in the view of NMFS) there is likely to be behavioral disturbance.

[6] For the deep and slope sites the calibration buoy was not anchored, and therefore drifted with the prevailing currents. A GPS receiver tracked the buoy location so that accurate ranges and azimuths to the ship could be calculated, and a depth gauge attached to the hydrophones allowed depth and any layback of the receiving sensors to be accounted for. Variations in hydrophone depth correlated well with observed wind speed and the movement of the buoy, as determined from its GPS. It was therefore possible to estimate the horizontal offset and direction of the hydrophone using a catenary model for the hydrophone and its cable. The deep site was shot in ~1600–1700 m water depth (Figure 2), and the sloped site was shot in ~600–1100 m water depth. The aim of the deep site calibration

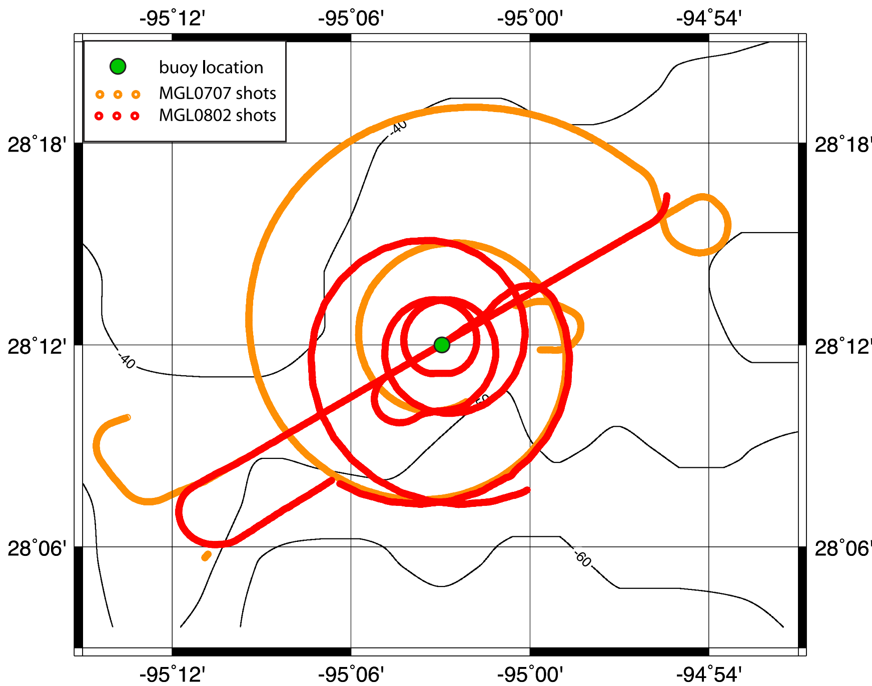

Figure 3. Site map for shallow calibration with bathymetry contours at 10 m intervals. The locations of shots recorded are shown in red (MGL0802) and orange (MGL0707), and the buoy location (anchored) is a green circle.

was to obtain measurements in water deep enough that the seafloor reflection is not a significant contributor to source levels. The aim of the slope site calibration was to study the character of this seafloor reflector and its contribution to sound exposure levels as the water depth changes.

[7] For the purposes of this paper, we describe the deep site results only out to ranges before the bottom reflections dominate so that it is essentially a proxy for very deep water settings, or an ocean half-space. Such environments are often encountered when surveys are conducted far from the shoreline, as in mid-ocean ridge or abyssal plain settings. For mitigation purposes, sloped sites can be treated as deep sites as long as the seafloor reflection does not exceed 160 dB referenced to 1 μPa (RMS), which for this area appears to occur at a depth of ~1700 m. However, sound propagation in this type of environment will be highly site specific and dependent on the local geology (reflectivity) of the seafloor.

[8] At the shallow site, the buoy was anchored to the seafloor, simplifying shooting patterns (Figure 3). The water depth at this site was ~40–50 m, creating an environment where sound is expected to reverberate in the water column, and the upper seafloor. In the shallow environment sound propagation will therefore also be highly dependent on the local seafloor geology.

3. R/V *Marcus Langseth* Seismic Source

[9] The R/V *Langseth* uses up to four strings of air gun subarrays (Figure 4). Each subarray is 16 m long, with nine active air guns and one ready spare. Thus, a total of up to 36 guns may be activated. For some experiments, particularly 3-D surveys, only two strings are used simultaneously, but here we focus on calibration results for the four string array, since this is the most commonly used and will represent the strongest source level. Relative to the two string array, the sound field of the four string array is simpler to characterize, since it is expected to be largely symmetrical, whereas the two string array will have more significant differences between sound levels in the fore and aft directions, as opposed to athwart ship. Seismic source arrays are intended to focus their energy downward toward the Earth and the scientific targets within. However, significant sound also propagates in near-horizontal directions which is where marine life typically hear the resulting sounds.

[10] The R/V *Langseth*'s 16-m-long subarrays are towed with a nominal horizontal separation of 6–8 m, and in the case of this experiment at a depth of

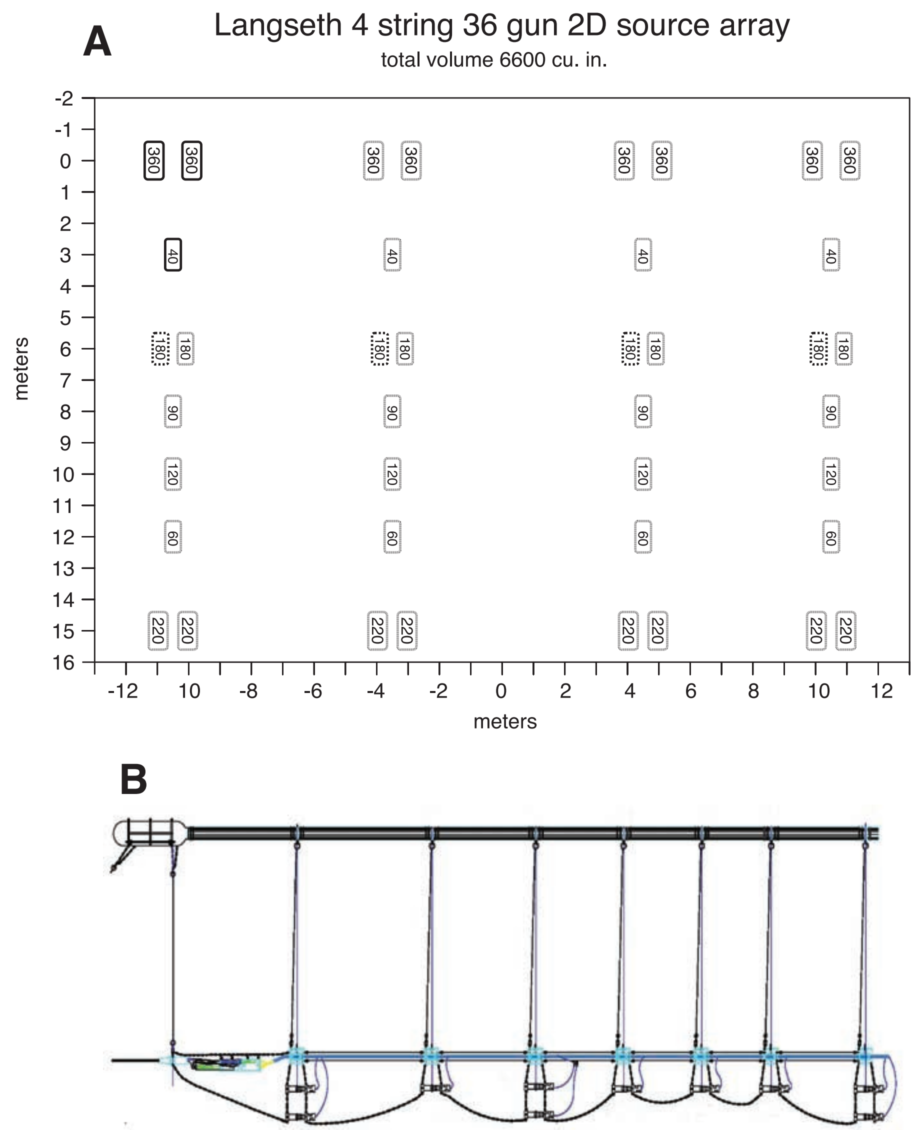

Figure 4. Schematic R/V *Langseth* gun array layout for the calibration experiment. The array comprises four identical but separately towed strings, each with ten air guns. (a) Each string is made up of three two-gun clusters and four individual guns. The purpose of the clusters is to provide a larger, more slowly reverberating residual air bubble (which improves overall array tuning) while at the same time reducing the amplitude of that bubble's reverberation, which further improves tuning. One of the 180 in^3 air guns within the central cluster is normally turned off and held in reserve as a spare. (b) Detailed side view of the towing arrangement for one of the four identical source strings on the R/V *Langseth*.

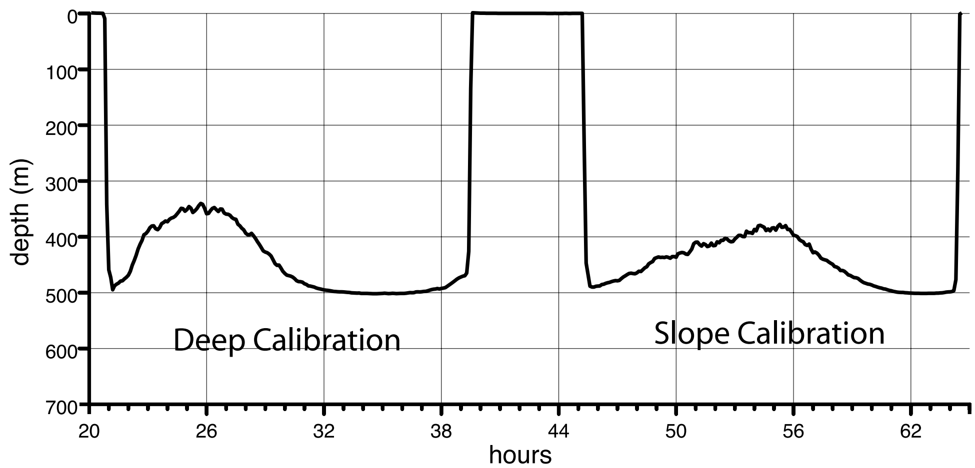

Figure 5. Depth gauge measurements from the deepest (500 m) hydrophone at the deep deployment site. Time is in hours on 30 and 31 January 2008.

6 m. The sound from each air gun arrives at a position in space following a delay time equal to the distance divided by the mean sound speed along that path. Only at large distances and only directly below the air gun arrays will the distance to all the guns be nearly the same such that the sound pulses add coherently together to produce one strong arrival. The standard measure of the source array's strength is achieved by converting this arrival's received (or modeled) level back to a notional distance of 1 m from the array's geometrical center. The resulting sound level (258.6 dB, as modeled for the R/V *Langseth* four-string array) is never physically achieved, but is nevertheless used as a representation of the source level. A hydrophone positioned off to one side of the ship's path, such that the sound is traveling roughly horizontally and in a direction 90° from the towing direction, will hear four pulses, one from each string. A receiver positioned at some horizontal distance *along* the ship's track will hear a combination of seven pulses generated by the pair of two-gun clusters and five individual air guns present within each subarray. At short ranges to the source, the pulses from the different air guns are spread out in time such that the peak pressures observed are the result of the summation of pulses from a few air guns, not the full array. At short ranges, the integral of the squared sound level (pressure) over time is much lower than it would be if all the pulses arrived simultaneously.

4. Instrumentation

[11] The seismic source was recorded using a spar buoy with two broadband hydrophones that recorded continuously during the experiment. For the shallow site, both hydrophones were deployed at 18 m. For the deep and sloped sites, one hydrophone was hung on a 500 m cable and the other on an 18 m cable. For the deep site results, only data from the deepest hydrophone are utilized, since this sensor recorded higher received levels at a given range. The deep phone was weighted with a 20 lb weight and had a pressure gauge attached to monitor true depth as the buoy drifted with the currents. True depth varied between ~350 and 500 m, because of variations in the vertical shear of the near surface current with changes in the wind and tides (Figure 5).

[12] The signals were detected using ITC-1042 spherical omnidirectional hydrophones with preamplifiers. The response of these sensors was calibrated to an accuracy of about 2dB at the Transdec facility in San Diego. The sensors provide useful data spanning a frequency range from a few Hz to 100 kHz. The two channels of hydrophone data were digitized with a National Instruments USB-9233 four-channel 24-bit data acquisition device. For this experiment, a sample rate of 50 kHz was used, providing information up to 25 kHz. The digitized data were recorded on a Samsung Q1 Ultra Mobile PC using a LabView interface, located in a watertight housing at the top end of the buoy. Absolute time was determined for the hydrophone data using GPS timing. GPS determined positions (used to track the surface position of the buoy) were transmitted to the ship using a Pacific Crest RFM96W radio operating at 450 MHz and were also recorded at the buoy. The individual components of the system were powered

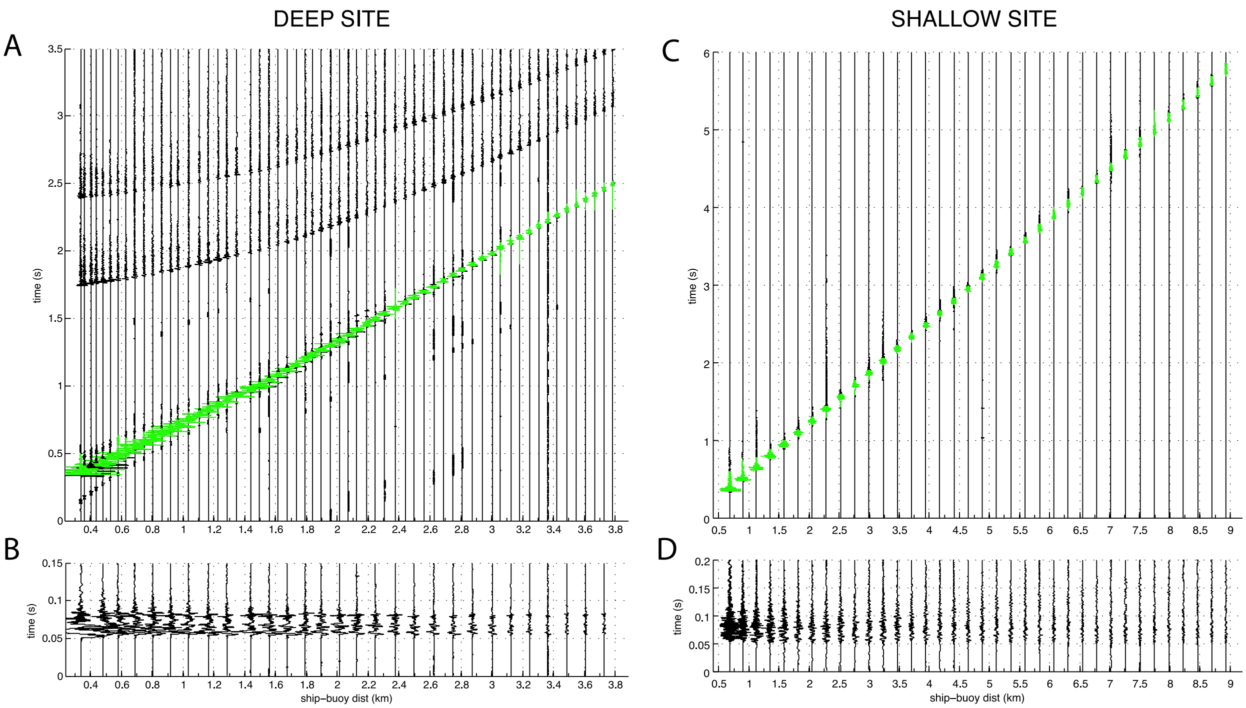

Figure 6. (a) Record section showing a subset of the waveforms from the deep site at the deep (500 m) hydrophone and (b) close-up of traces aligned on the first arrival. The area of the waveform in green illustrates the 5–95% window on the direct arrival used for the RMS calculation. The low-amplitude signal slightly preceding the direct arrival at closest ranges is believed to be cross talk from the signal on the shallow hydrophone. Arrivals due to seafloor reflections can be seen 0.5 to 2 s after the direct arrival. Bubble pulses add to the duration of the main signal. (c) Record section showing a subset of the waveforms from the shallow site and (d) close-up of traces aligned on the first arrival. The area of the waveform in green illustrates the 5–95% window on the direct arrival used for the RMS calculation. Reverberations from the seafloor make the initial part of the arrival less impulse and higher frequency than the deep site. Contributions to the reverberations likely come from both the water column bounces and reflections from within the near surface sediment layers.

separately using on board rechargeable battery packs.

5. Analysis Methods

[13] Acoustic received levels were quantified using root-mean-square (RMS) and sound exposure level (SEL) calculations. In the U.S.A. the current standard for mitigation is RMS; however, there is debate on whether or not this is the best measurement to use with impulsive air gun sources and if it accurately represents what a marine mammal might be sensitive to [e.g., *Madsen*, 2005].

[14] The RMS amplitude, typically expressed as dB referenced to 1 μPa, is a measure of the average pressure over the duration of the pulse. It is calculated as the square root of the sum of the squared pressures within a given time window and therefore depends on the selection of this window and its duration. Here we define the time window as that containing 90% of the cumulative pulse energy, a common approach in marine mammal studies [e.g., *Blackwell et al.*, 2004; *Madsen*, 2005]. This is determined by initially integrating the signal over a 0.5 s window that encompasses the entire arrival, as well as some period of noise before and after. The 5% and 95% cumulative energy levels are identified from this analysis and used to define a new window for the RMS calculation. Figure 6 shows record sections of waveforms from the deep and shallow sites, with the windows used to calculate the RMS highlighted in green. The goal in this procedure is to capture and accurately represent the amount of acoustic energy flux that might impact an animal's environment, while also recognizing that there are species-dependent time windows that define a single exposure to anthropogenic sound [cf. *Green*, 1985]. The 90% RMS levels determined by this procedure are quite dependent upon signal character [*Madsen*, 2005; *Madsen et al.*, 2006] and this may introduce

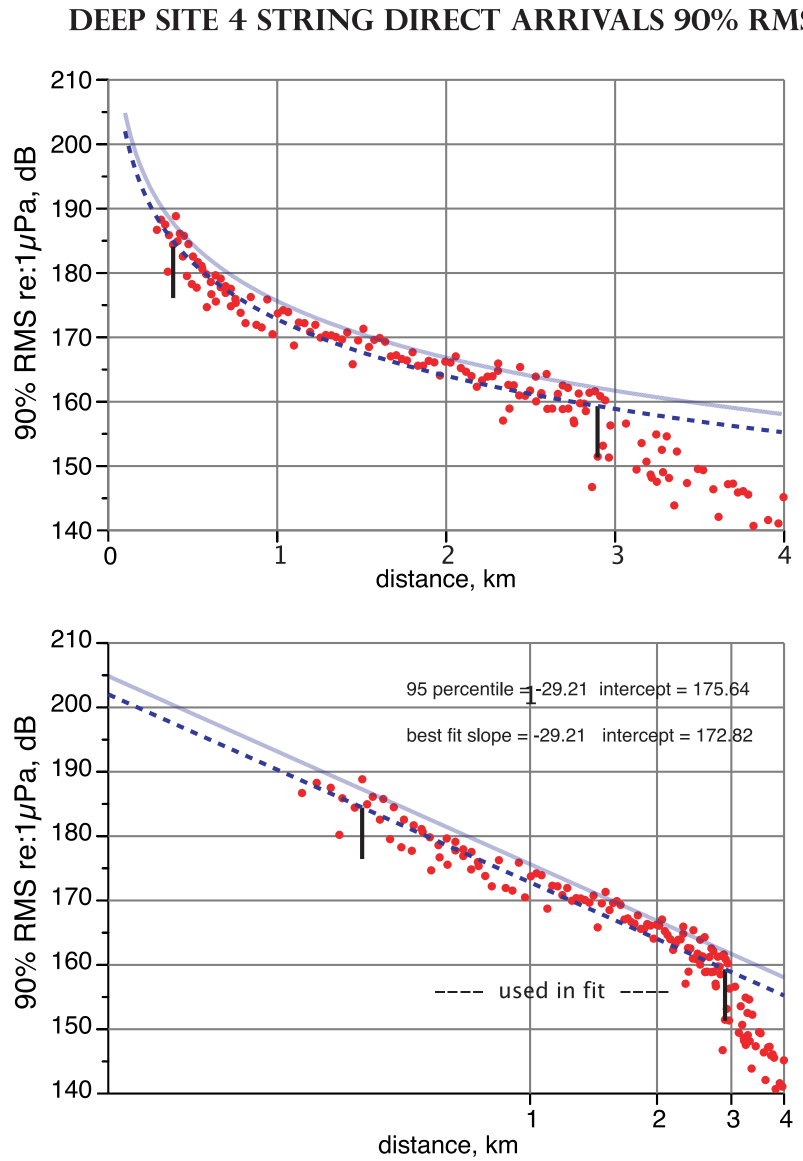

Figure 7. RMS referenced to 1 μPa values for direct arrivals of the four-string array at the deep site versus distance displayed on (top) linear and (bottom) $\log_{10}$ scales. Curves showing a least squares fit to the data and marking the 95th percentile levels are shown as dashed and solid lines, respectively. Slope is dB/decade, and intercept is at 1 km.

unwanted scatter into the results. Therefore, a determination of energy flux within a fixed time window may more accurately define exposure to noise.

[15] This same 90% energy window is used to estimate the SEL of the arrival. SEL is a measure of the energy flux density of an arrival, defined as the product of signal intensity and duration [*Young*, 1970]. Its decibel value (dB referenced to 1 Pa^2s) will equal the RMS decibel amplitude if calculated for a 1 s duration window: $SEL_{(dB)} = RMS_{(dB)} + 10 \log_{10}(T)$, where T is the RMS integration time in seconds [*Madsen*, 2005]. For signals with durations <1 s, as expected for an air gun pulse, the SEL value will be less than the RMS.

[16] To estimate the distance required for sound levels to fall off to any given value of regulatory significance, it is common to adopt a precautionary “95th percentile” approach (W. J. Richardson, LGL Ltd., personal communication, 2008). A best fit line for received level versus distance is determined, and then shifted upward until 95% of the data points fall below it. For direct and/or shallow

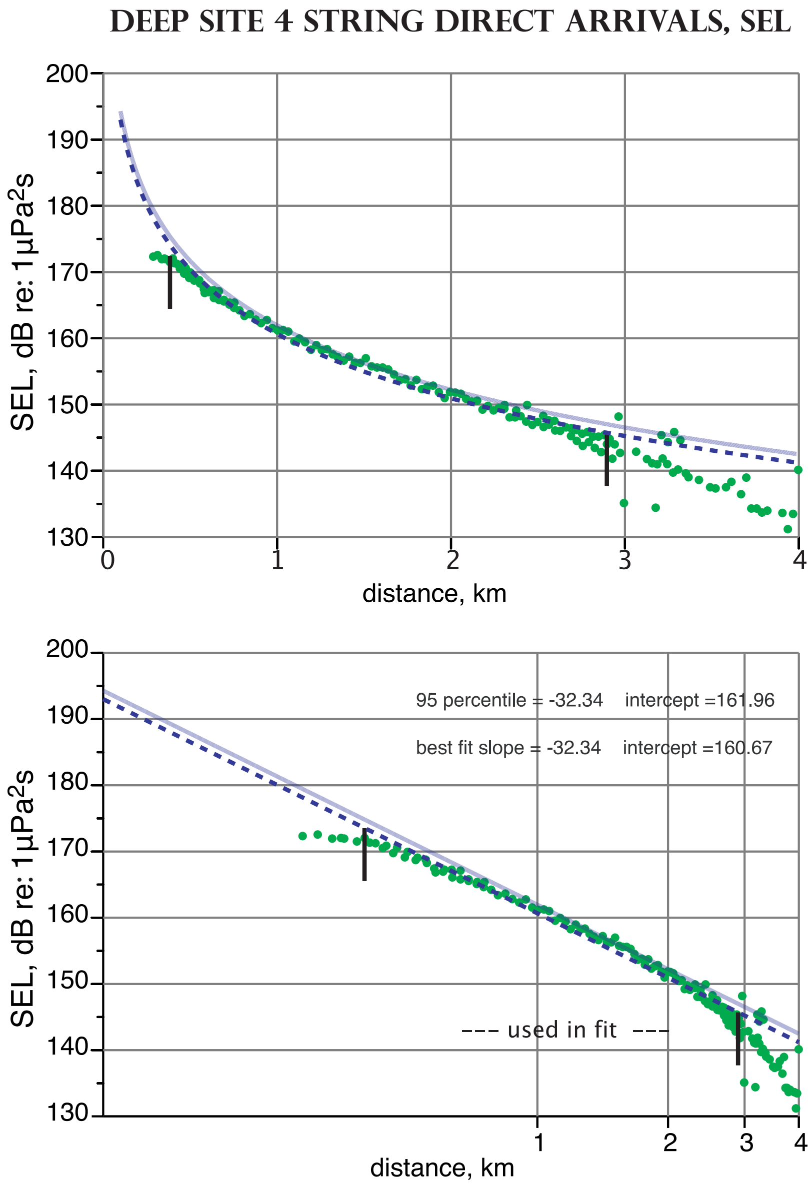

Figure 8. SEL referenced to 1 $\mu Pa^2 s$ values for direct arrivals of the four-string array at the deep site versus distance displayed on (top) linear and (bottom) $\log_{10}$ scales. Curves showing a least squares fit to the data and marking the 95th percentile levels are shown as dashed and solid lines, respectively. Slope is dB/decade, and intercept is at 1 km.

arrivals, "best fit" obeys the equation Received level (dB) = intercept + slope * $\log_{10}$(offset).

6. Results

6.1. Deep Site

[17] For the deep site, only the direct arrivals are included. Seafloor reflections, which may become significant at greater distances are not considered. The deep site therefore represents a half-space or "true deep" such as would be expected in water that was deep enough for seafloor reflections not to rise above 160 dB RMS referenced to 1 μPa. The sites for which this is true will depend on both the water depth and the seafloor geology (reflectivity).

[18] In Figures 7 and 8, RMS and SEL received levels, respectively, are shown as a function of distance from the center of array. Note that the difference between RMS and SEL values at the same range is ~14 dB at this site, though it increases slightly with distance. The safety criteria and radii results are summarized in Table 1. These empirically determined ranges are based on a linear fit to the data in log-log space (i.e., dB received

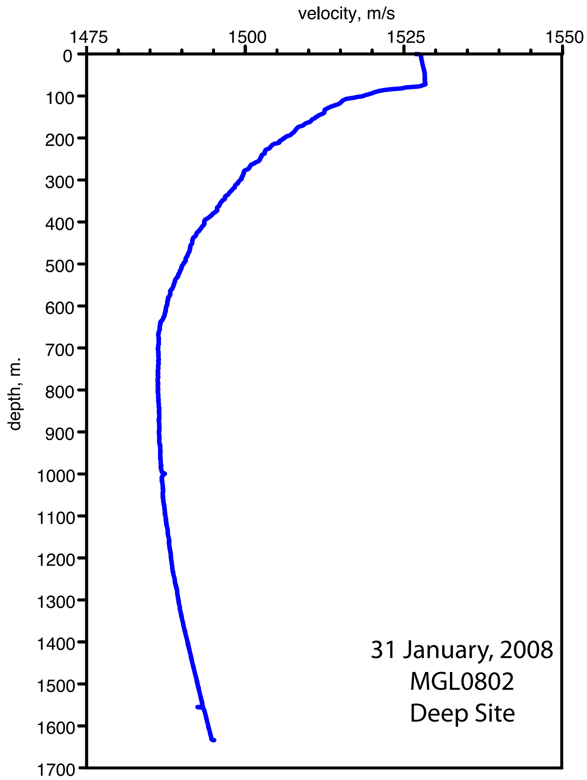

Figure 9. XBT profile for deep water site show sound velocity variations with water depth. The velocity profile is fairly typical for deep ocean, with a thin (< 100 m) surface layer of high velocity above a broad deep low-velocity elbow known as the Sound Fixing and Ranging (SOFAR) channel with a lowest velocities around 650 m. This velocity profile causes sound energy from a surface source to refract downward.

level versus $\log_{10}$ of the distance in km) and an equivalent curve encompassing the 95th percentile of the measurements. The fall off of received levels in the SEL data in the near field relative to the model curves shows that the array behaves like multiple discrete sources rather than a single source at distances <1 km. The falloff at ranges >2.5 km is associated with downward refraction due to the sound velocity profile as illustrated in XBT data collected at the deep site (Figure 9). (The warmer surface layer leads to downward refraction at most ocean sites). This means that 160 dB radii obtained from the best fitting curves represent overestimates at small and large distances for this hydrophone depth. For example, while the Table 1 shows a calculated 160 dB RMS referenced to 1 μPa level at 3.4 km for the 95th percentile fit, Figure 7 shows that there are in fact no arrivals above 160 dB RMS referenced to 1 μPa beyond 3 km range.

6.2. Shallow Site

[19] For the shallow site, inline and side shots are differentiated by color in Figures 10 and 11 (RMS and SEL, respectively). The data show that for the four-string array there is not a significant azimuthal dependence in received levels, with only slightly elevated sound levels recorded athwart ship. The difference between RMS and SEL at similar ranges for this site is ~8 dB with the difference decreasing slightly with increasing range. The results summarized in Table 1 indicate larger exposure radii when compared with the deep site. This is consistent with the reverberation of energy reflecting between the sea surface and seafloor. Similar to the deep site, the 160 dB referenced to 1 μPa RMS radius derived from the best fitting curve overestimates the required distances, as received levels drop off slightly at the more distance ranges. While Table 1

Table 1. Exposure Radii for R/V *Langseth* Four-String Seismic Sources

Received Level Thresholds	Exposure Radii (km)	
	Deep Site	Shallow Site
RMS (dB Referenced to 1 μPa), 95th Percentile Fit		
190	0.3	0.5
180	0.7	1.6
170	1.6	5.2
160	3.4[a] (3)	17.5[a] (16)
RMS (dB Referenced to 1 μPa), Best Fit		
190	0.3	0.3
180	0.6	1.1
170	1.2	3.7
160	2.7	12.5
SEL (dB Referenced to 1 μPa²s), 95th Percentile Fit		
190	N/A	N/A
180	0.3[a] (N/A)	0.6
170	0.6	2.2
160	1.2	8.5
150	2.3	32.6[b]
SEL (dB Referenced to 1 μPa²s), Best Fit		
190	N/A	N/A
180	0.3[a] (N/A)	0.4
170	0.5	1.5
160	1.0	5.6
150	2.1	21.7[b]

[a] Levels are overestimated (on the basis of slope fit) because of falloff in energy at furthest and closest ranges. Conservative estimates based on data shown in Figures 7–10 are given in brackets. N/A indicates that these dB levels are unlikely to be achieved because of falloff in energy at the closest ranges.
[b] Levels are based on calculations, as there are no observations at these ranges. However, they are likely overestimated because of the falloff observed at further ranges.

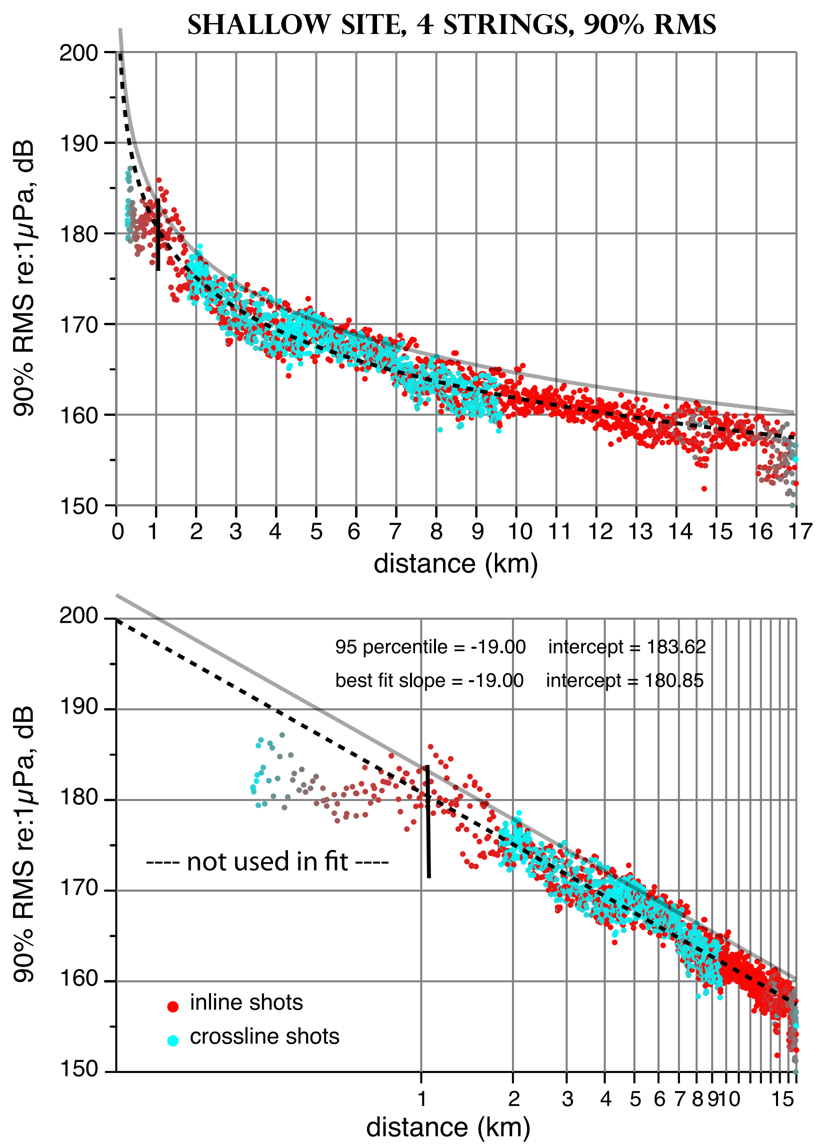

Figure 10. RMS referenced to 1 μPa values for arrivals of the four-string array at the shallow site versus distance displayed on (top) linear and (bottom) $\log_{10}$ scales. Curves showing a least squares fit to the data and marking the 95th percentile levels are shown as dashed and solid lines, respectively. Slope is dB/decade, and intercept is at 1 km. Inline shots are shown in red, and cross-line (athwart ship) shots are shown in cyan, with intermediate shading for shots between these azimuth extremes.

shows a calculated 160 dB referenced to 1 μPa RMS level at 17.5 km for the 95th percentile fit, Figure 10 shows that there are in fact no arrivals above 160 dB referenced to 1 μPa RMS past ~16 km.

6.3. Overall Sound Exposure of Buoy

[20] Another way to consider SEL levels with respect to potential impact on marine mammals is to look at cumulative SEL [e.g., *Madsen et al.*, 2006]. Cumulative SEL considers the overall sound level exposure associated with a particular period of time, or experiment. In this case we have summed the SEL values for the 2007 shallow site experiment, the 2008 shallow site experiment and the 2008 deep site experiment separately (Figure 12). This is an imperfect measure of a theoretical exposure level for a marine mammal over the course of an experiment, because it assumes that the animal would not move to avoid the sound source, and it also does not account for the fact that the source would be shut down if the animal was observed within the 180 dB safety radii. These closest shots, which would be least likely to be experienced by a marine mammal, have the most significant contribution to the signal as illustrated

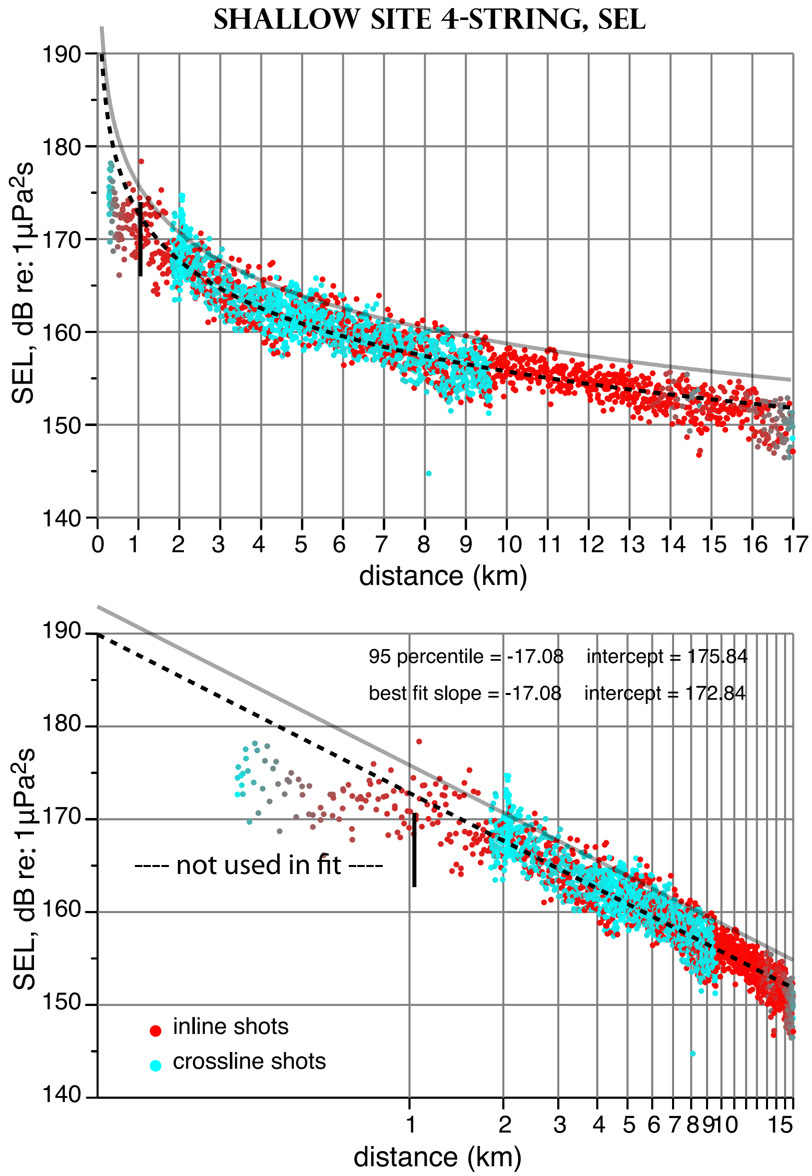

Figure 11. SEL referenced to 1 μPa^{2}s values for arrivals of the four-string array at the shallow site versus distance displayed on (top) linear and (bottom) $\log_{10}$ scales. Curves showing a least squares fit to the data and marking the 95th percentile levels are shown as dashed and solid lines, respectively. Slope is dB/decade, and intercept is at 1 km. Inline shots are shown in red, and cross-line (athwart ship) shots are shown in cyan, with intermediate shading for shots between these azimuth extremes.

by the steeper slope in the cumulative level when the ship is close to the buoy. If shots within the 180 dB safety radii are excluded in this calculation, overall sound exposure drops by between 1 and 9 dB. Nevertheless, the calculation gives a sense for the potential overall exposure level associated with an experiment by measuring the overall sound level exposure at the buoy.

6.4. Spectral Content

[21] Figures 13 and 14 show spectra for shots at ranges of ~0.3 km and ~1 km, respectively. Both energy spectral density and 1/3rd octave levels are shown for shots at the shallow (18 m hydrophone) and deep (500 m hydrophone) sites. Energy spectral density is an appropriate measurement for pulsed or transient signals, and 1/3rd octave levels are most relevant for marine mammal hearing [*Richardson et al.*, 1995]. At the shallow water site, the low-frequency energy is suppressed compared to the high-frequency energy because acoustic wavelengths become sufficiently long that the low-frequency waves from the source interact strongly with the bottom. Much of the spectral

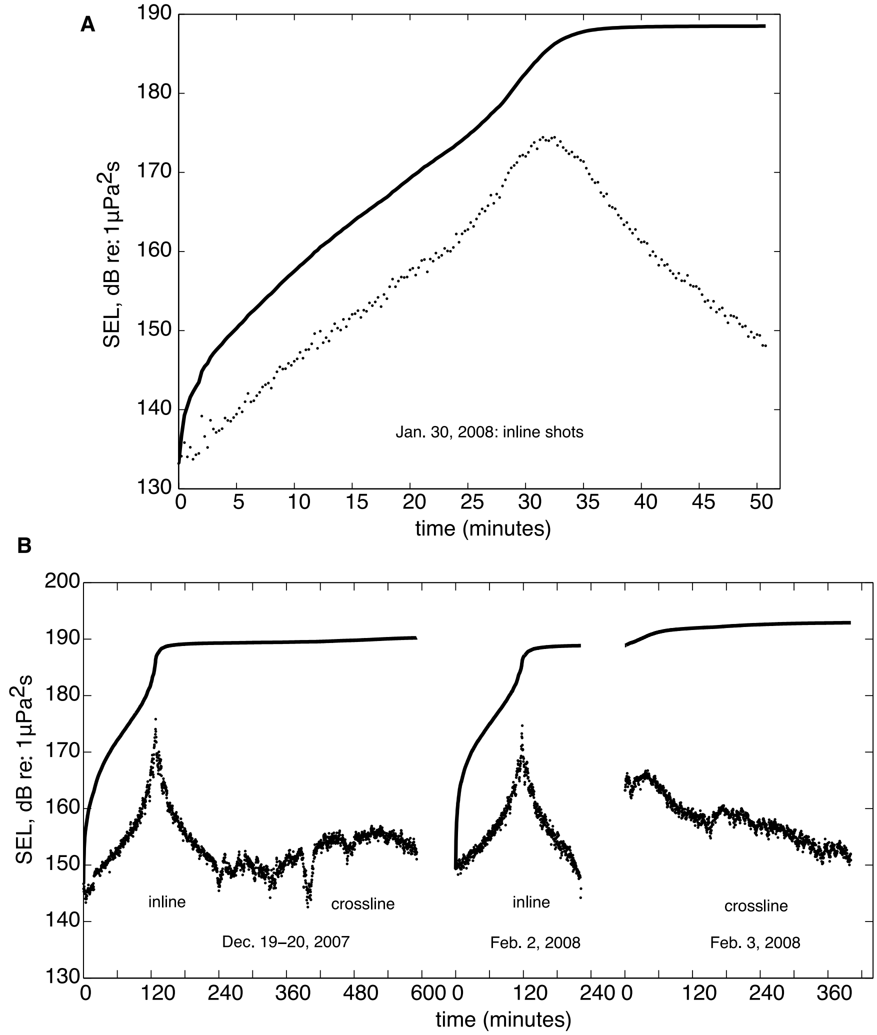

Figure 12. Overall cumulative SEL referenced to 1 μPa^{2}s through time for the (a) deep and (b) shallow sites. The shallow site is separated out into the work conducted in 2007 and the work conducted in 2008. SEL levels for individual shots through time are shown as black dots, with the cumulative level of those shots shown as black lines. Time is shown in minutes relative to the first shot of the different experiments.

level difference between the deep and shallow water sites at higher frequencies may be a consequence of differences in total range to the source (the sites are at the same horizontal range, but different slant ranges) and partly because the surface reflected pulse is not included in the analysis of the deep water data.

7. Conclusions

[22] Recommended safety radii for the full four-string array of the R/V *Langseth* are below the levels that have been used to date based on modeling [e.g., *Diebold et al.*, 2006]. The data confirm significantly different propagation loss rates in shallow and deep water as previously observed for the R/V *Ewing* [*Tolstoy et al.*, 2004], with lower loss rates in shallow water.

[23] Notably, the difference between RMS and SEL received dB levels, while often thought of as a fixed offset, is seen to be highly dependent on water depth, as well as variable with distance. Specifically in shallow water the difference is ∼8 dB whereas for deep water the difference is ∼14 dB. This is reasonable, because reverberations in the shallow arrivals mean that the 90% RMS integration window is longer, whereas deep arrivals are more impulsive and therefore have a shorter integration window.

[24] Source characteristics for air gun arrays are often specified according to an exploration industry

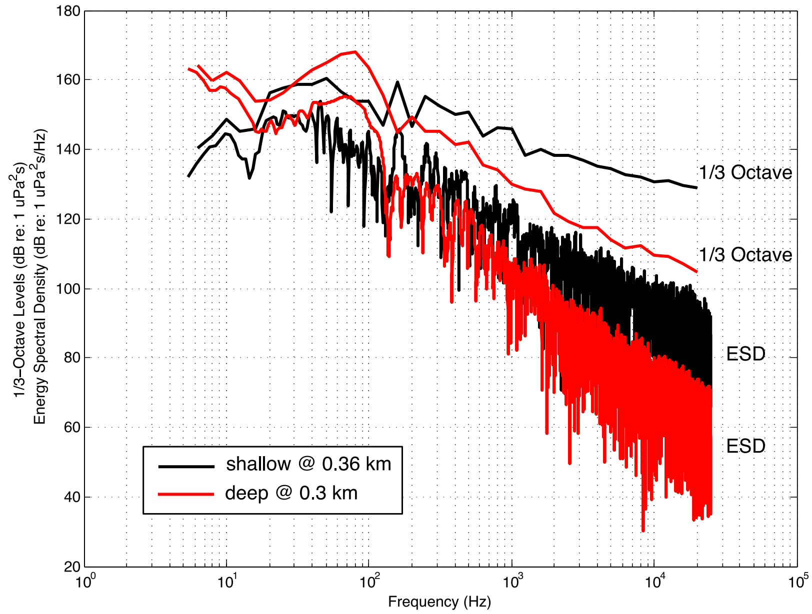

Figure 13. Comparison of spectra for two shots recorded at nearby ranges (0.3–0.36 km) but different water depths. The shallow site shot (black) is at 0.36 km and the deep site shot (red) is at 0.3 km from the buoy. Both energy spectral density (bottom traces) and 1/3rd octave levels (top traces) are shown.

standard [*Johnston et al.*, 1998]. One of the key elements in this specification is the peak source level (in decibels) that represents its power as measured at a distance of one meter from the center of the source array. This level is never actually achieved when the source is an array of multiple air guns separated in space. Instead the number is estimated by model or measurement at a large distance and back projected mathematically to a notional distance of 1 m. Following this standard, the R/V *Langseth* four-string array source peak level is 258.6 dB.

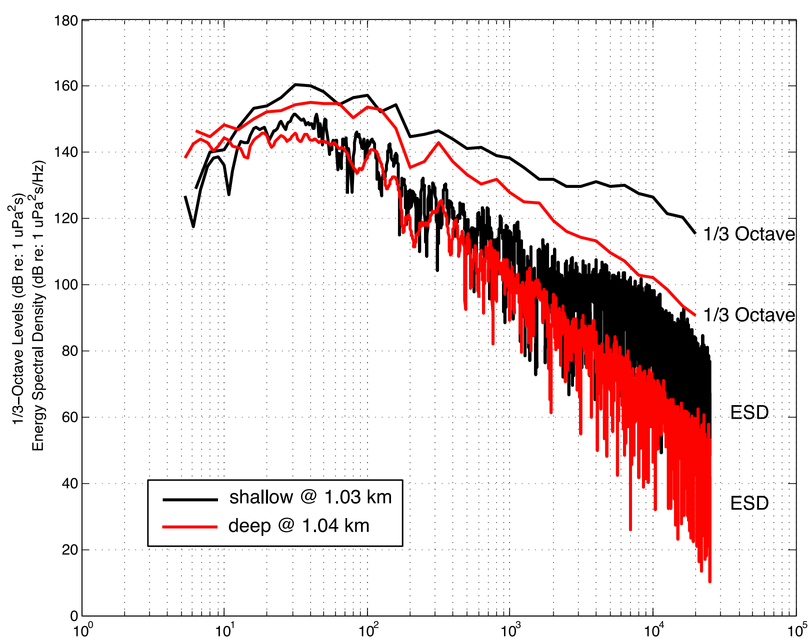

Figure 14. Comparison of spectra for two shots recorded at ranges slightly over 1 km but in different water depths. The shallow site shot (black) is at 1.03 km and the deep site shot (red) is at 1.04 km from the buoy. Both energy spectral density (bottom traces) and 1/3rd octave levels (top traces) are shown.

[25] When compared with calibration results from the largest 20-element array (∼8500 cubic inches, back-projected 258 dB peak source level) deployed on the now-retired R/V *Ewing*, exposure radii at the deep site increase slightly in the far field (for received levels of 160 dB referenced to 1 μPa RMS), possibly reflecting more densely spaced data. At the shallow site, the safety radii decrease in the near field (for received levels of 190, 180 and 170 dB referenced to 1 μPa RMS), consistent with a better tuned array with smaller guns; however, they increase slightly in the far field (for received levels of 160 dB referenced to 1 μPa RMS), where field measurements were lacking for the R/V *Ewing* calibration. Data for the 2003 *Ewing* calibration were significantly more sparse than the data collected here, often relying on single points to draw conclusions. The dense spacing of data for the R/V *Langseth* calibration allows for a more sophisticated understanding of the structure of the sound field and more robust estimates of received sound levels. However, we also note that seafloor geology can have a significant effect on received levels, particularly at shallow depths, and differences at shallow depths between R/V *Ewing* and R/V *Langseth* results may also be due to different sites.

[26] Spectra show a broadband signal, with energy from a few Hz to many kHz, but with all but a small fraction of the total energy being concentrated in the 10–300 Hz range.

Acknowledgments

[27] We thank the captains and crews of R/V *Langseth* for legs MGL0707 and MGL0802, as well as D. Stroup and P. Monigle for their assistance at sea. This work was conducted in conformance with an Incidental Harassment Authorization issued to L-DEO by the National Marine Fisheries Service under provisions of the U.S. Marine Mammal Protection Act. We thank the associate editor, Peter Tyack, John Richardson, and an anonymous reviewer for comments that significantly improved the manuscript. This work was supported by the National Science Foundation under grant OCE-0624599. This paper is LDEO contribution number 7279.

References

Blackwell, S. B., J. W. Lawson, and J. T. Williams (2004), Tolerance by ringed-seals (*Phoca hispida*) to impact pile driving and construction sounds at an oil production island, *J. Acoust. Soc. Am.*, *115*, 2346–2357, doi:10.1121/1.1701899.

Breitzke, M., O. Boebel, S. El Naggar, W. Jokat, and B. Werner (2008), Broad-band calibration of marine seismic sources used by *R/V Polarstern* for academic research in polar regions, *Geophys. J. Int.*, *174*, 505–524, doi:10.1111/j.1365-246X.2008.03831.x.

Diebold, J. B., M. Tolstoy, P. J. Barton, and S. P. Gulick (2006), Propagation of exploration seismic sources in shallow water, *Eos Trans. AGU*, *87*(36), Jt. Assem. Suppl., Abstract OS41A-03.

Gordon, J., D. Gillespie, J. Potter, A. Frantzis, A. P. Simmonds, R. Swift, and D. Thompson (2004), A review of the effects of seismic surveys on marine mammals, *Mar. Technol. Soc. J.*, *37*, 16–34.

Green, D. M.(1985), Temporal factors in psychoacoustics, in *Time Resolution in Auditory Systems*, edited by A. Michelson, pp. 120–140, Springer, New York.

Johnston, R. C., D. H. Reed, and J. F. Desler (1998), SEG standards for specifying marine seismic energy sources, *Geophysics*, *53*, 566–575.

Madsen, P. T. (2005), Marine mammals and noise: Problems with root mean square sound pressure levels for transients, *J. Acoust. Soc. Am.*, *117*, 3952–3957, doi:10.1121/1.1921508.

Madsen, P. T., M. Johnson, and P. J. O. Miller (2006), Quantitative measures of air-gun pulses recorded on sperm whales (*Physeter macrocephalus*) using acoustic tags during controlled exposure experiments, *J. Acoust. Soc. Am.*, *120*, 2366–2379, doi:10.1121/1.2229287.

Richardson, W. J., C. R. Greene, C. I. Malme, and D. H. Thompson (1995), *Marine Mammals and Noise*, Academic, San Diego, Calif.

Tashmukhambetov, A. M., G. E. Ioup, J. W. Ioup, N. A. Sidorovskaia, and J. J. Newcomb (2008), Three-dimensional seismic array characterization study: Experiment and modeling, *J. Acoust. Soc. Am.*, *123*, 4094–4108, doi:10.1121/1.2902185.

Tolstoy, M., J. B. Diebold, S. C. Webb, D. R. Bohnenstiehl, E. Chapp, R. C. Holmes, and M. Rawson (2004), Broadband calibration of the *R/V Ewing* seismic sources, *Geophys. Res. Lett.*, *31*, L14310, doi:10.1029/2004GL020234.

Tyack, P. L. (2008), Implications for marine mammals of large-scale changes in the marine acoustic environment, *J. Mammal.*, *89*, 549–558, doi:10.1644/07-MAMM-S-307R.1.

Young, R. W. (1970), On the energy transported with a sound pulse, *J. Acoust. Soc. Am.*, *47*, 441–442, doi:10.1121/1.1911547.